PROCEEDINGS OF THE ROYAL SOCIETY A

Proc. R. Soc. A (2007) **463**, 551–568
doi:10.1098/rspa.2006.1776
Published online 18 October 2006

Novel phenomena-based dynamic model of carbon black/composite vapour sensors

By James W. T. Yates*, Michael J. Chappell and Julian W. Gardner

School of Engineering, University of Warwick, Coventry CV4 7AL, UK

A novel physically based mathematical model of carbon black/polymer vapour sensors is described, which incorporates parameters that have physical meaning. This model has an analytical solution and so requires negligible computational power to analyse a sensor's response to a particular form of input. Another advantage of this modelling approach is that the environmental dependencies of sensor responses may be compensated for and so help in the design of better pattern-recognition algorithms for electronic nose systems. This also means that the underlying chemistry of the sensors may be decoupled from their physical non-analyte specific properties. Experimentally, three different conducting nanocomposite polymers, poly(styrene-*co*-butadine), poly(ethyl-*co*-vinyl acetate) and poly(caprolactone), were tested. Each experiment consisted of separate exposures of the sensors to acetone and ethanol vapour in ambient air. A total of 336 such experiments were performed over a two-week period. The model was validated with respect to these data and was then fitted to the two vapour responses simultaneously, demonstrating its applicability to 'real world' systems. The temperature dependence of the model parameters was judged to be the most important factor and it needs to be compensated for when applying this type of sensor in practice.

Keywords: dynamic modelling; sensor modelling; parameter estimation; environmental conditions

1. Introduction

It is evident that for many applications, the dynamic responses of chemoresistor sensors hold a great deal of information. Previously, researchers have attempted to exploit this information using black box modelling or shape analysis, by convolution with standard functions, such as exponentials (Gardner *et al.* 1998). However, these are purely data-driven techniques and the resulting models provide little or no interpretation as far as the internal processes of the sensor are concerned. It would be beneficial, for practical applications, to separate the physical aspects of the sensor response from the chemical aspects[1]. This would

* Author and address for correspondence: AstraZeneca, Alderley Park, Cheshire SK10 4TG, UK (james.yates@astrazeneca.com).

[1] It is assumed that the chemical aspects provide discriminatory information, whereas the physical aspects do not.

Received 10 March 2006
Accepted 5 September 2006

help to enable pattern-recognition algorithms to correct automatically for changes in sensor response owing to environmental (Koscho *et al.* 2002) and device-to-device variations. It is apparent that a greater understanding of these effects would greatly help in the design of more robust electronic nose systems. The work reported in this article concerns a dynamic analysis of the processes that occur in a particular class of resistive gas sensors and the effect that environmental conditions have on these processes.

Composite polymer sensors take advantage of the change of polymer chain conformation when a polymer dissolves into a solvent (Flory 1953). The polymer is blended with fine carbon nanospheres with a diameter of *ca* 50 nm, which makes the composite material an electrical conductor when the carbon content is above a threshold value ρ_c. During absorption, the distances between nanospheres alter and so a change in film conductance is observed. These sensors undergo three effects: diffusion through the polymer film; chain conformation changes; and resultant conductivity changes. It is evident from the earlier studies that such sensors are greatly affected by both temperature and humidity (Covington 2001).

A model was developed to encompass the operating principles of this type of sensor. The free parameters within the model characterize the underlying physical and chemical aspects of the sensor operation. An automated electronic nose system was developed to produce data under different environmental conditions. These conditions were dictated by the ambient environment in order to simulate the operating conditions of a 'real' electronic nose system.

2. The model

The system modelled is that of a single resistive nanocomposite carbon black/polymer sensor in an atmosphere carrying a particular solvent vapour. The resistance of the polymer composite film is observed indirectly by using it as a resistive element in a potential divider circuit. The model developed actually predicts the current flowing through the sensor as a function of time. Its chemical and electrical properties are coupled to simulate the observed change in electrical response. This single sensor model is then used as a template to model an array of six sensors reacting to two different vapours in air. The model is constructed such that while the chemistry of interaction may be assumed to be specific only to the solvent and the polymer being examined, the conductance changes are specific to the individual sensor and are dependent upon its geometry and manufacturing process.

The model is inherently one dimensional owing to two assumed symmetries; these being that the concentration of the solvent is constant across the surface of the sensor and that the electric field is constant in the direction parallel to the sensor electrodes. These assumptions greatly simplify the chemo-electric calculations and are justified owing to the geometry of the sensor and the experimental conditions under which the model is used. Experimental observations have suggested that diffusion is not driven linearly by the concentration gradient. Evidence includes a sharp diffusion front followed by a constant concentration (Windie 1984; Parker & Vesely 1986). The diffusion equations adapted from heat transport assume that all the concentrations are equally likely, that is, that the medium allows concentrations that can tend to

infinity. However, swelling of the polymer described in §1, along with associated thermodynamic changes, rules out this possibility. It is clear that these results suggest a concentration-dependent diffusion rate.

An electron-hopping model is assumed for conductivity changes. Electron hopping takes place in the absence of physical contact between the granules. Here, an electrical potential difference exists between the granules. Thus, this model considers microscopic phenomena, namely electron transfer between two conducting nanospheres, and extends them to a macroscopic level by appealing to effective medium theory (Böttger & Bryksin 1985).

As with all models, some assumptions have to be made. It is argued that the following are both necessary and reasonable assumptions to make: necessary, as they provide a baseline for the allowing order to generate a mathematically tractable model; and reasonable, as any variation between the real situation and the assumptions below would produce small-scale effects.

(i) The composite material is homogeneous and isotropic. This means that diffusion will progress in the same manner throughout the polymer and the integrals taken below to calculate current flow are valid.
(ii) Diffusion is a reversible process in the sense that the purge stage will leach all the solvent molecules from the polymer. This implies that there is no permanent reactive process, only an absorption process.
(iii) Only one chemical species is present in the solvent and there is no molecule-to-molecule interaction.
(iv) The solvent molecules are spherical. This is because a generic model is required and this assumption simplifies the modelling process.

A first approximation to the diffusion process is to set up a linear diffusion model with two regions of high and low concentrations of solvent molecules with corresponding high and low diffusion rate constants. It will be shown that this assumption provides a sharp diffusion front. In the following analysis: medium 1 (all with subscripts 1) denotes the swollen polymer and medium 2 (all with subscripts 2) is taken to be the atmosphere. Subscript p represents unswollen polymer regions. The time-dependent position of the interface between the atmosphere and the polymer is denoted by $X_1(t)$ and the concentration front in the polymer by $X_{\mathrm{p}}(t)$. Note that the concentration profile in the atmosphere is of little interest, but is present to provide boundary conditions and the moving interface X_2. The system equations are specified thus

$$\frac{\partial c_1}{\partial t} = D_1 \frac{\partial^2 c_1}{\partial x^2}, \tag{2.1}$$

$$\frac{\partial c_2}{\partial t} = D_2 \frac{\partial^2 c_2}{\partial x^2}, \tag{2.2}$$

$$\frac{\partial c_{\mathrm{p}}}{\partial t} = D_{\mathrm{p}} \frac{\partial^2 c_{\mathrm{p}}}{\partial x^2}. \tag{2.3}$$

Here, D_1,D_{p} are the diffusion constants in the polymer for high and low concentrations, respectively; D_2 is the diffusion constant in air; and c (with appropriate subscript) is the temporal and spatially dependent solvent

concentration, i.e. in the polymer

$$D(c_1) = \begin{cases} D_\mathrm{p} & \text{if } c_1(x) < C_X, \\ D_1 & \text{if } c_1(x) \geq C_X, \end{cases} \tag{2.4}$$

where C_X is the diffusion rate threshold condition. The initial and boundary values are set as

$$D_1 \left(\frac{\partial c_1}{\partial t} \right)_{x_1 = X_1} - D_2 \left(\frac{\partial c_2}{\partial t} \right)_{x_2 = X_2} + c_0 Q \frac{\mathrm{d}X_1}{\mathrm{d}t} = 0, \tag{2.5}$$

$$D_1 \left(\frac{\partial c_1}{\partial t} \right)_{x_1 = X_\mathrm{p}} - D_\mathrm{p} \left(\frac{\partial c_\mathrm{p}}{\partial t} \right)_{x_1 = X_\mathrm{p}} = 0, \tag{2.6}$$

where Q is the gas to polymer partition coefficient and the boundary and initial values are specified to be

$$\begin{aligned} c_2(0, t) &= c_0, \\ c_2(X_2, t) &= c_0, \\ c_2(-\infty, t) &= 0, \\ c_1(X_1, t) &= c_0 Q, \\ c_\mathrm{p}(-\infty, t) &= 0, \\ c_1(X_\mathrm{p}, t) &= C_X, \end{aligned} \tag{2.7}$$

where X_p represents the position of the diffusion front within the polymer film.

This form of diffusion is well studied and a good review may be found in Crank (1975). Figure 1 shows a schematic of this; the diffusion rate alters as solvent molecules diffuse through the surface of the polymer. The thickness of the polymer is initially assumed to be infinite as we first consider a semi-infinite medium.

In accordance with the assumption that the interface moves owing to the influx of the solvent vapour, this movement is expressed as

$$\frac{\mathrm{d}X_1}{\mathrm{d}t} = S \left\{ D_1 \left(\frac{\partial c_1}{\partial x_1} \right)_{x_1 = X_1} + c_1(X_1) \frac{\mathrm{d}X_1}{\mathrm{d}t} \right\}. \tag{2.8}$$

Here, in both equations, the first term in the bracket represents flux across the interface owing to concentration gradient and the second represents flux owing to interface moving relative to the diffusing substance. S is the coefficient of proportionality between flux and linear expansion of the polymer. The particular solution is of the following form (Carslaw & Jaeger 1959):

$$c_1(x, t) = C_1 + A \left[\mathrm{erf} \left[\frac{x_1}{2(D_1 t)^{1/2}} \right] - \mathrm{erf} \left[\frac{X_\mathrm{p}}{2(D_1 t)^{1/2}} \right] \right], \tag{2.9}$$

$$c_2(x, t) = C_2 + B\mathrm{erf} \left[\frac{x_2}{2(D_2 t)^{1/2}} \right], \tag{2.10}$$

$$c_p(x, t) = C_\mathrm{p} + G\mathrm{erfc} \left[\frac{x_1}{2(D_\mathrm{p} t)^{1/2}} \right], \tag{2.11}$$

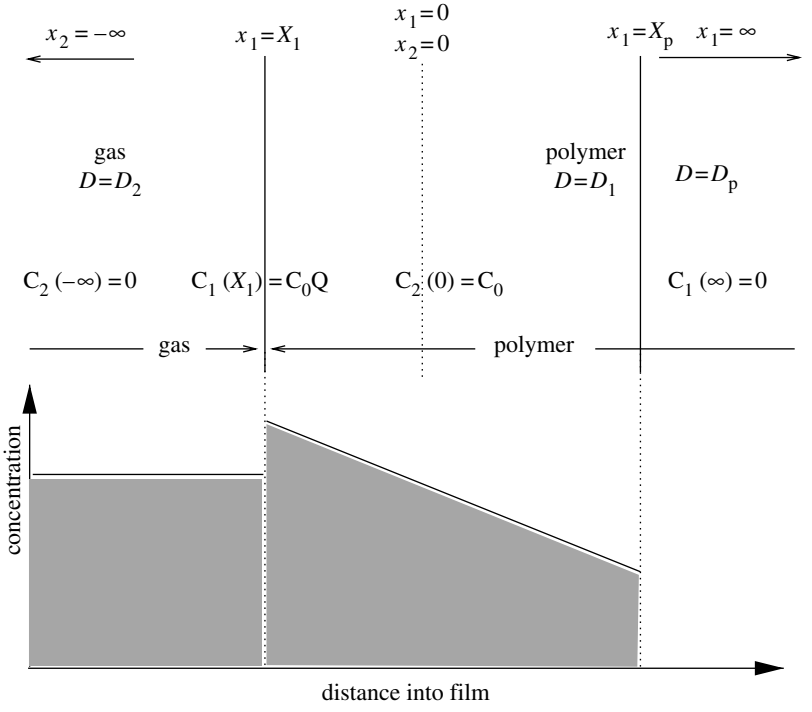

Figure 1. Illustration of variable diffusion rate model.

where A, B, G, C_1, C_2, C_p are parameters whose values are to be determined from the boundary and the flux conditions.

3. Analysis of the model

A particular analytical solution to the above specified boundary problem is now sought. This is then simplified to a case which may be easily simulated.

(*a*) *Semi-infinite medium*

Given the candidate solutions (2.9–2.11), the conditions under which they satisfy the boundary value problem above are analysed. Note first that equations (2.1–2.3) are satisfied as the error function is a standard solution of diffusion equation for the initial conditions. Applying the boundary conditions (2.7) yields

$$c_1(X_1, t) = c_0 Q = C_1 + A\left[\operatorname{erf}\left[\frac{X_1}{2(D_1 t)^{1/2}}\right] - \operatorname{erf}\left[\frac{X_p}{2(D_1 t)^{1/2}}\right]\right], \tag{3.1}$$

$$c_p(X_p, t) = C_X = \frac{1}{2} C_p \left(1 + \operatorname{erf}\left[\frac{X_p}{2(D_p t)^{1/2}}\right]\right), \quad \text{for all } t \geq 0. \tag{3.2}$$

It is also deduced that

$$C_1 = C_X, \tag{3.3}$$

$$C_2 = c_0, \tag{3.4}$$

$$B = c_0, \tag{3.5}$$

$$C_\mathrm{p} = -2G. \tag{3.6}$$

For equations (3.1) and (3.2) to hold, it is necessary that

$$X_1 = 2\alpha(D_1 t)^{1/2}, \tag{3.7}$$

$$X_\mathrm{p} = 2\beta(D_1 t)^{1/2}, \tag{3.8}$$

which implies that

$$C_\mathrm{p} = \frac{2C_X}{1 + \mathrm{erf}\left[\left(D_1^{1/2}\beta\right)/D_2^{1/2}\right]}. \tag{3.9}$$

Finally equations (2.5), (2.8), (3.7), (3.8) and (3.1) yield

$$c_0 Q - C_X = A\left[\mathrm{erf}\left(\left(\frac{D_2}{D_1}\right)^{1/2}\frac{Sc_0}{\pi^{1/2}}\right) - \mathrm{erf}(\beta)\right], \tag{3.10}$$

and

$$\alpha = \left(\frac{D_2}{D_1}\right)^{1/2}\frac{Sc_0}{\pi^{1/2}}. \tag{3.11}$$

Thus, from equations (3.2) and (3.10), one can obtain

$$A = \frac{c_0 Q - C_X}{\left[\mathrm{erf}\left((D_2/D_1)^{1/2}(Sc_0)/\pi^{1/2}\right) - \mathrm{erf}(\beta)\right]}. \tag{3.12}$$

Therefore, all parameters, except β, can be expressed in terms of the initial conditions and the diffusion constants. However, substituting equations (3.12) and (3.9) into the flux condition (2.6) yields

$$\frac{c_0 Q - C_X}{[\mathrm{erf}((D_2/D_1)^{1/2}(Sc_0)/\pi^{1/2}) - \mathrm{erf}(\beta)]} D_1^{1/2}\exp(-\beta^2) + \cdots$$

$$\cdots + \frac{C_X}{\mathrm{erf}\,\beta(D_1/D_2)^{1/2}} D_\mathrm{p}^{1/2}\exp\left(-\beta^2\left(\frac{D_1}{D_\mathrm{p}}\right)\right) = 0, \tag{3.13}$$

which is an equation in β alone. However, it is apparent that this equation is transcendental, and therefore, it has to be solved numerically for β.

(*b*) *Finite medium with sharp diffusion front*

The polymer film is now assumed to be of finite thickness, y_0, so that the domain of the polymer is the interval $[-y_0, 0]$ initially. Hence, to move to consideration of a finite medium, the following condition in equation (2.7) is modified to give

$$c_{\mathrm{p}}(-y_0, t) = 0. \tag{3.14}$$

The following is also assumed in order to permit an analytical solution to the finite medium problem to be found:

$$D_{\mathrm{p}} = 0. \tag{3.15}$$

This condition stops rapid transport of the solvent vapour beyond the base of the polymer film. Hence, the flux condition at the X_{p} boundary becomes (Crank 1975)

$$-A\left(\frac{D_1}{\pi t}\right)^{1/2} \exp\left(-\frac{X_{\mathrm{p}}^2}{4D_1 t}\right) = C_X \frac{\mathrm{d}X_{\mathrm{p}}}{\mathrm{d}t}. \tag{3.16}$$

Assuming the same form for the boundary, X_{p}, as in equation (3.8) the following is deduced,

$$\frac{-2A}{C_X \pi^{1/2}} = \beta \exp[\beta^2], \tag{3.17}$$

and in the notation used above (2.11)

$$C_{\mathrm{p}} = -G\mathrm{erf}\left[\frac{-y_0}{2(D_{\mathrm{p}} t)^{1/2}}\right]. \tag{3.18}$$

This means that $c_{\mathrm{p}}(x, t) = 0$ is the only possible solution of the form (2.11), which is to be expected, given that the diffusion rate is zero in this region.

(*c*) *Steady-state solutions in the swollen polymer*

One simplification that will prove beneficial when calculating the current between the electrodes of the sensor is the assumption of a quasi-steady state in the swollen region of the polymer.

Taking the initial and boundary conditions (2.7) as before, an approximate solution in the swollen region of the polymer is proposed to be (Crank 1975)

$$c_1(x, t) = [c_0 Q - C_X]\left[\frac{X_{\mathrm{p}} - x}{X_{\mathrm{p}} - X_1}\right] + c_X. \tag{3.19}$$

It is immediately obvious that this expression satisfies the initial conditions (2.7). The flux conditions at X_1 and X_{p} need to be satisfied and so equation (2.5) implies that

$$-D_1[c_0 Q - C_X]\frac{1}{X_{\mathrm{p}} - X_1} + c_{\mathrm{p}}\left(\frac{D_{\mathrm{p}}}{\pi t}\right)^{1/2} \exp\left(-\frac{X_{\mathrm{p}}^2}{4D_{\mathrm{p}} t}\right) = 0, \tag{3.20}$$

which is entirely consistent using the expressions for X_1 and X_p given in equations (2.5) and (3.8).

To ascertain the value of β, one has to take into account the boundary conditions and the steady-state solution (3.19). Let $\Sigma_c(t)$ be the total amount of solvent in the polymer body as predicted by equation (3.19), so that

$$\Sigma_c(t) = \frac{1}{2}[Qc_0 + C_X][X_1(t) - X_p(t)]. \tag{3.21}$$

Then the amount of solvent absorbed at the boundary X_1 must be given by $\Sigma_c(t)$, i.e.

$$\frac{1}{2}[Qc_0 + C_X]\left[\frac{dX_1}{dt} - \frac{dX_p}{dt}\right] = Qc_0\frac{dX_1}{dt}. \tag{3.22}$$

By substituting equations (3.7) and (3.8) in equation (3.22), we obtain

$$\beta = -\frac{1}{2}\frac{Qc_0}{C_X}\alpha. \tag{3.23}$$

The constant α is known from conditions at the polymer/atmosphere interface (3.11) and so β can be determined from equation (3.23). Thus, it can be seen that β is uniquely determined.

The linear expression (in x) in equation (3.19) is only an approximation; it does not satisfy the diffusion equation itself. However, the quasi-steady-state approximation has been used in a number of studies to a great effect (Islam *et al.* 2002; Ficker 2003).

4. Conduction within the composite material

A nearest neighbour electron-hopping Mott-type model is considered for the relationship between local concentration and conductivity. This is of the form (Rubin *et al.* 1999)

$$\sigma = \sigma_0 \exp(-\chi_s), \tag{4.1}$$

where σ is the conductivity of the polymer; σ_0 is the conductivity of the polymer in air; and χ_s is a function of the local swelling factor. By assuming small concentrations of vapour ($\chi_s \approx 0$), equation (4.1) may be linearized to obtain

$$\sigma \approx \sigma_0(1 - \chi_s). \tag{4.2}$$

In this model, it is assumed that χ_s is proportional to the volume change, ΔV_p, which is proportional to the local solvent concentration, c. Thus, χ_s may be written as

$$\chi_s = Nc, \tag{4.3}$$

where N is a constant.

To calculate the current, i, flowing between the two electrodes of the homogenous sensor, it is necessary to integrate the conductivity against the electric field, E, over the surface, L, bisecting the electrodes as follows:

$$i = \int_L \sigma E dL. \tag{4.4}$$

With the geometry of a finite film, the electric field E is (Gardner *et al.* 1989)

$$E(0,y) = \frac{V}{\pi}\left[(y+y_0)^2 - \frac{w^2}{4}\right]^{-(1/2)}, \tag{4.5}$$

because in the reference frame of the diffusion model, the surface of the film is (initially) at $x=0$ and the electrodes are at $x=-y_0$. If, with reference to equations (3.7) and (3.8), we set

$$X_1(t) = k_1 t^{1/2}, \tag{4.6}$$

$$X_\mathrm{p}(t) = k_\mathrm{p} t^{1/2}, \tag{4.7}$$

then assuming quasi-steady state, as in equation (3.19), the integral (4.4) can be evaluated to give

$$\begin{aligned} i = \frac{\sigma_0}{\pi}\Bigg[& N(c_0 Q - C_X)\frac{1}{(k_1-k_\mathrm{p})t^{1/2}}[k_\mathrm{p}t^{1/2}[\cosh^{-1}(k_1 t^{1/2}+y_0) \\ & -\cosh^{-1}(k_\mathrm{p}t^{1/2}+y_0)] - [\exp(\cosh^{-1}(k_1 t^{1/2}+y_0)) \\ & -\exp(\cosh^{-1}(k_\mathrm{p}t^{1/2}+y_0)) - y_0[\cosh^{-1}(k_1 t^{1/2}+y_0) \\ & -\cosh^{-1}(k_\mathrm{p}t^{1/2}+y_0)]]] - \log 2y_0 - NC_X\cosh^{-1}(k_\mathrm{p}t^{1/2}+y_0)+1]\Bigg]. \end{aligned} \tag{4.8}$$

5. Experimental method

The test rig used is a simple electronic nose rig and its basic design has been tested in many experiments (Covington *et al.* 2001) with success. This test requires the production of some odour external to the nose and transport to the sensor where the odour is detected.

(*a*) *Sensors and sensor chamber*

The sensor chamber uses a narrow channel with the sensors set to be flush with one side. The resulting flow, for velocities in the range used in experiments described in this section, is approximately laminar with a parabolic profile. The exact dimensions of the channel were arrived at after a number of prototypes were tested. The aim of this device is to produce a plug-type laminar flow in order to eliminate mixing dynamics.

The sensor chamber is capable of housing and performing measurements on six resistive sensors simultaneously. Three polymers in pairs were studied. These polymers were: poly(caprolactone) (PCL); poly(styrene-*co*-butadine) (PSB); and poly(vinyl acetate) (PVA). The reasons for using two sensors of each polymer are: built-in redundancy means that the experiment does not have to stop if one of the polymer devices fail; the chemical characteristics of each sensor pair are assumed to be common and thus may be determined more accurately; and the decoupling of chemical and physical aspects of the response can be demonstrated more effectively.

The carbon black/polymer sensors used in this experiment were produced in-house by the Sensors Research Laboratory, School of Engineering, University of Warwick. The sensor films were fabricated to have 5% carbon black by weight and film thicknesses of *ca* 50 μm were produced. Two chemical compounds—similar in polarity and mass—were chosen (i.e. ethanol and acetone) to represent a reasonably challenging discriminatory problem faced by an e-nose system. Temperature and humidity sensors (SHT71, Sensirion, Zurich, Switzerland) were mounted near the sensor chamber in order to measure environmental conditions. This enabled an investigation into the effect of these conditions on the parameters studied within the sensor response model.

(*b*) *Experimental regime*

The model requires that the boundary concentration is constant and instantaneous. It also implicitly assumes that the ambient humidity and temperature, and the temperature of the sensor bodies are all constant for the duration of a response measurement. This is implicit owing to the hypothesized dependence of the parameter values upon these conditions.

A test sequence consists of two solvent exposures: one to acetone and one to ethanol vapour in air. This allows for a more rigorous validation of the model by fitting the two responses simultaneously. Thus, each experiment involves firstly a fresh air 'purge' and then an acetone exposure; this is followed by a second fresh air purge and an ethanol exposure. Typically, the ethanol and the acetone vapour concentrations will be 100–500 p.p.m. The experimental rig recorded the voltage change across a potential divider, of which a sensor formed a resistive element. This measurement was converted to the current flowing through the sensor prior to parameter estimation.

6. Computer implementation

Model optimization was carried out within the commercial MATLAB v. 5.3 software environment. A genetic algorithm (Yates 2004) was used to search for candidate optimal models. The Levenberg–Marquardt algorithm used for final parameter tuning has already been implemented in MATLAB as the LSQNONLIN routine. This routine requires the start values of parameters, the function to minimize and the stopping criteria as input arguments. It outputs the fitted parameters, the fitting error and whether successful convergence has occurred.

Common to both of these optimization stages was the simulation script which produced, based upon specific parameters values, a simulation of two sets of six sensors representing the six experimental sensors reacting to the two solvents. The two sets of six responses for each experiment are interrelated. It is set that pairs of sensors share the same chemical characteristics and that between two exposures a sensor retains the same physical characteristics.

The sum of squared errors $E(\hat{\boldsymbol{p}})$ with respect to the experimental error was weighted using the range of each time-series in order to obtain a uniform fit over the various sensor responses. The outline of the technique used to process the experimental data was as follows. The earliest experimental data were processed using the best guess found using the genetic algorithm as start values for the

Levenberg–Marquardt algorithm. The resulting estimated parameters were then recorded in a table, along with the recorded environmental data. The estimated parameter results were then used for the second experiment's start values. This process of using final values of the previous experiment as start values for the next was continued until the model had been fitted to all the data.

It was considered that this strategy represented the most efficient way to process the data. In addition, any concern that this process would cause a propagation of errors was removed when the results demonstrated that this was not the case. It was assumed that the environment in the laboratory would vary continuously with time and that, consequently, the model parameters would vary continuously with time. Using the results of the previous experiment, parameter values supplied a 'best' start parameter vector for the next experiment. This should minimize the number of iterations of the Levenberg–Marquardt algorithm necessary to complete the task.

7. The identified model

For parameter estimation, C_X was set to $(1/2)Qc_0$. This was found to give the best fit by trial and error. This assumption was made in order to reduce the number of parameters for identification. Figure 2 shows an example of the model fit compared with the real data, and the change in current is plotted so that all of the responses may be viewed on the same scale. The model fitted well to the experimental data, with respect to the sum of squares of the residual errors. The experimental and simulated data are plotted in the same shade of grey for each sensor. This fit has a weighted sum of squared errors of 1.944. The error was measured with respect to the magnitude of response and so an average pointwise error of 4.5% was estimated. This is considered to be very good, given that the constraints on the parameters and the model to fit all 12 responses simultaneously, the order of magnitude difference of the response to acetone and ethanol, and the data were noisy.

There is some oscillatory behaviour apparent in the experimental data. It is thought that this was owing to slight variations in the atmospheric concentration of the test solvent, brought about by fluid flow in the fluidic system of the test rig. They are of much smaller magnitude than the overall change in sensor current flow and so are not thought to prove problematic for model validation and parameter estimation.

Table 1 details the estimated parameter values for this fit as well as the standard deviations. The parameter estimate standard deviations were calculated using the Hessian matrix method detailed in Marsili-Libelli *et al.* (2003). It can be seen that the parameters do give an insight into the speed and the magnitude of sensors' responses to the two solvents. Judging by the values of k_{p_i} and k_{1_i}, the PCL sensor appears to produce the fastest response to acetone, whereas the PVA sensor reacts quickest to ethanol. For magnitude of response, it appears that PSB has the greatest magnitude of response overall (judging by values for the parameter N). It should also be noted that all the parameters have standard deviations of an order of magnitude lower than their respective estimates, thus giving high confidence in the values estimated.

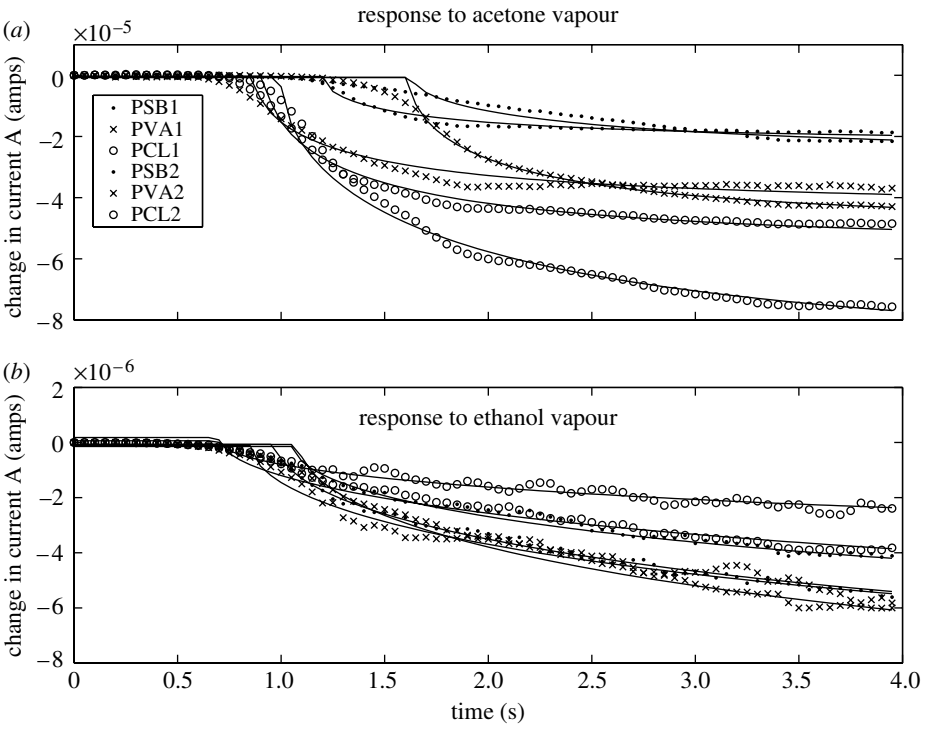

Figure 2. Example of the model fitted to an experimental dataset.

8. Results

The rate constants in the model relate to the progress of the solvent diffusion front through the polymer films. It would be expected that there is a strong environmental relationship owing to mass action and the fact that a temperature dependence of sensor responses has been observed before (Covington *et al.* 2000). Figure 3 shows the results of the estimated parameter values when the model is fitted to each of the experiments.

It can be seen that there is a much stronger temperature relationship with the acetone responses (figures 3*a*,*c*,*e*) than with the ethanol responses (figures 3*b*,*d*,*f*). This is probably owing to the much stronger acetone responses recorded. The dependences are either linear or slightly 'sigmoidal' in shape. There is high scatter in some parts of the plot and it is thought that this is owing to poor automatic fits for some of the experimental responses. All of the data are reported here rather than arbitrary censoring.

In the proposed model, only the product NQc_0 is estimable, which can be seen by examining equation (4.8). This is proportional to the total change in sensor current, as can be seen by inspecting equation (4.8).

Figure 4 shows the dependence of the product NQc_0 on temperature. It can be seen that there is a consistent growth or reduction with temperature. Previously, only a reduction has been observed (Covington *et al.* 2000).

However, it must be remembered that in the previous studies, only the sensor temperature was varied while the solvent concentration remained static. In the case of the system considered here, solvent concentration is a function of

Table 1. Estimated parameter values, where s.d. stands for standard deviation. Parameters are labelled $P_{\text{solvent, sensor}}$ or P_{sensor}. For sensors: 1, PCL; 2, PSB; 3, PVA. For solvents: 1, acetone; 2, ethanol. Parameters are as in equation (4.8). For example, c_1 represents the concentration of acetone.

parameter	units	value	s.d.	parameter	units	value	s.d.
$k_{p_{11}}$	$\mathrm{ms}^{-1/2}$	2.5×10^{-3}	3.2×10^{-5}	$k_{1_{11}}$	$\mathrm{ms}^{-1/2}$	2.1×10^{-4}	2.7×10^{-13}
$k_{p_{21}}$	$\mathrm{ms}^{-1/2}$	2.1×10^{-3}	2.4×10^{-10}	$k_{1_{21}}$	$\mathrm{ms}^{-1/2}$	8.0×10^{-5}	4.5×10^{-23}
$k_{p_{12}}$	$\mathrm{ms}^{-1/2}$	4.3×10^{-4}	1.4×10^{-7}	$k_{1_{12}}$	$\mathrm{ms}^{-1/2}$	3.1×10^{-4}	3.8×10^{-12}
$k_{p_{22}}$	$\mathrm{ms}^{-1/2}$	1.2×10^{-4}	2.7×10^{-8}	$k_{1_{22}}$	$\mathrm{ms}^{-1/2}$	2.5×10^{-4}	2.3×10^{-15}
$k_{p_{13}}$	$\mathrm{ms}^{-1/2}$	3.0×10^{-3}	3.2×10^{-5}	$k_{1_{13}}$	$\mathrm{ms}^{-1/2}$	1.2×10^{-4}	1.0×10^{-28}
$k_{p_{23}}$	$\mathrm{ms}^{-1/2}$	3.1×10^{-2}	3.8×10^{-9}	$k_{1_{23}}$	$\mathrm{ms}^{-1/2}$	7.0×10^{-3}	1.2×10^{-19}
N_{11}	M^{-1}	2.7×10^{0}	1.2×10^{-4}	Q_{11}	none	4.7×10^{0}	4.1×10^{-8}
N_{21}	M^{-1}	7.5×10^{-1}	2.0×10^{-5}	Q_{21}	none	2.3×10^{-1}	1.8×10^{-6}
N_{12}	M^{-1}	1.5×10^{0}	3.7×10^{-6}	Q_{12}	none	3.6×10^{0}	3.4×10^{-6}
N_{22}	M^{-1}	1.47×10^{0}	1.1×10^{-4}	Q_{22}	none	5.7×10^{-1}	3.5×10^{-6}
N_{13}	M^{-1}	4.7×10^{-3}	2.1×10^{-5}	Q_{13}	none	6.9×10^{-4}	1.3×10^{-9}
N_{23}	M^{-1}	5.4×10^{-1}	2.5×10^{-6}	Q_{23}	none	1.0×10^{-1}	1.1×10^{-7}
y_1	m	1.4×10^{-4}	1.7×10^{-5}	σ_1	$\mathrm{Av}^{-1}\,\mathrm{m}^{-1}$	1.4×10^{0}	2.2×10^{-16}
y_2	m	1.0×10^{-5}	7.1×10^{-5}	σ_2	$\mathrm{Av}^{-1}\,\mathrm{m}^{-1}$	3.1×10^{-2}	9.1×10^{-15}
y_3	m	2.1×10^{-4}	5.7×10^{-6}	σ_3	$\mathrm{Av}^{-1}\,\mathrm{m}^{-1}$	2.3×10^{0}	5.5×10^{-14}
y_4	m	1.4×10^{-4}	2.5×10^{-8}	σ_4	$\mathrm{Av}^{-1}\,\mathrm{m}^{-1}$	1.4×10^{0}	3.6×10^{-16}
y_5	m	1.5×10^{-4}	7.3×10^{-5}	σ_5	$\mathrm{Av}^{-1}\,\mathrm{m}^{-1}$	1.5×10^{0}	1.2×10^{-14}
y_6	m	2.5×10^{-4}	7.1×10^{-6}	σ_6	$\mathrm{Av}^{-1}\,\mathrm{m}^{-1}$	2.5×10^{-4}	1.6×10^{-13}
c_1	M	1.1×10^{-1}	1.6×10^{-7}	c_2	M	1.2×10^{-1}	9.3×10^{-6}

temperature as well, owing to the temperature dependence of partition coefficients. This is a more realistic finding as 'in the field' electronic noses sample at ambient temperature.

Thus, there are two partitions interacting: that for the sample chamber liquid/vapour partition and that for the sensor/vapour partition. By Trouton's law (Patrash &Zellers1993), we have that

$$Q_{\mathrm{L}} = A_{\mathrm{L}}\mathrm{e}^{B_{\mathrm{L}}T}, \tag{8.1}$$

$$Q_{\mathrm{S}} = A_{\mathrm{S}}\mathrm{e}^{B_{\mathrm{S}}T}, \tag{8.2}$$

where Q_{L}, Q_{S} are the partition coefficients for the sample and the sensor chambers, respectively, and T is the temperature. Therefore, $Q_{\mathrm{S}}c_0$, the concentration at the atmospheric boundary, is given by

$$Q_{\mathrm{S}}c_0 = \frac{Q_{\mathrm{S}}c_{\mathrm{L}}}{Q_{\mathrm{L}}}, \tag{8.3}$$

$$Q_{\mathrm{S}}c_0 = c_{\mathrm{L}}\frac{A_{\mathrm{S}}}{A_{\mathrm{L}}}\mathrm{e}^{(B_{\mathrm{S}}-B_{\mathrm{L}})T}, \tag{8.4}$$

where c_{L} is the sample chamber liquid concentration (which is assumed to be constant). It can be seen that an increase or decrease with temperature of the boundary condition Qc_0 is dependent upon the relative sizes of B_{S} and B_{L}.

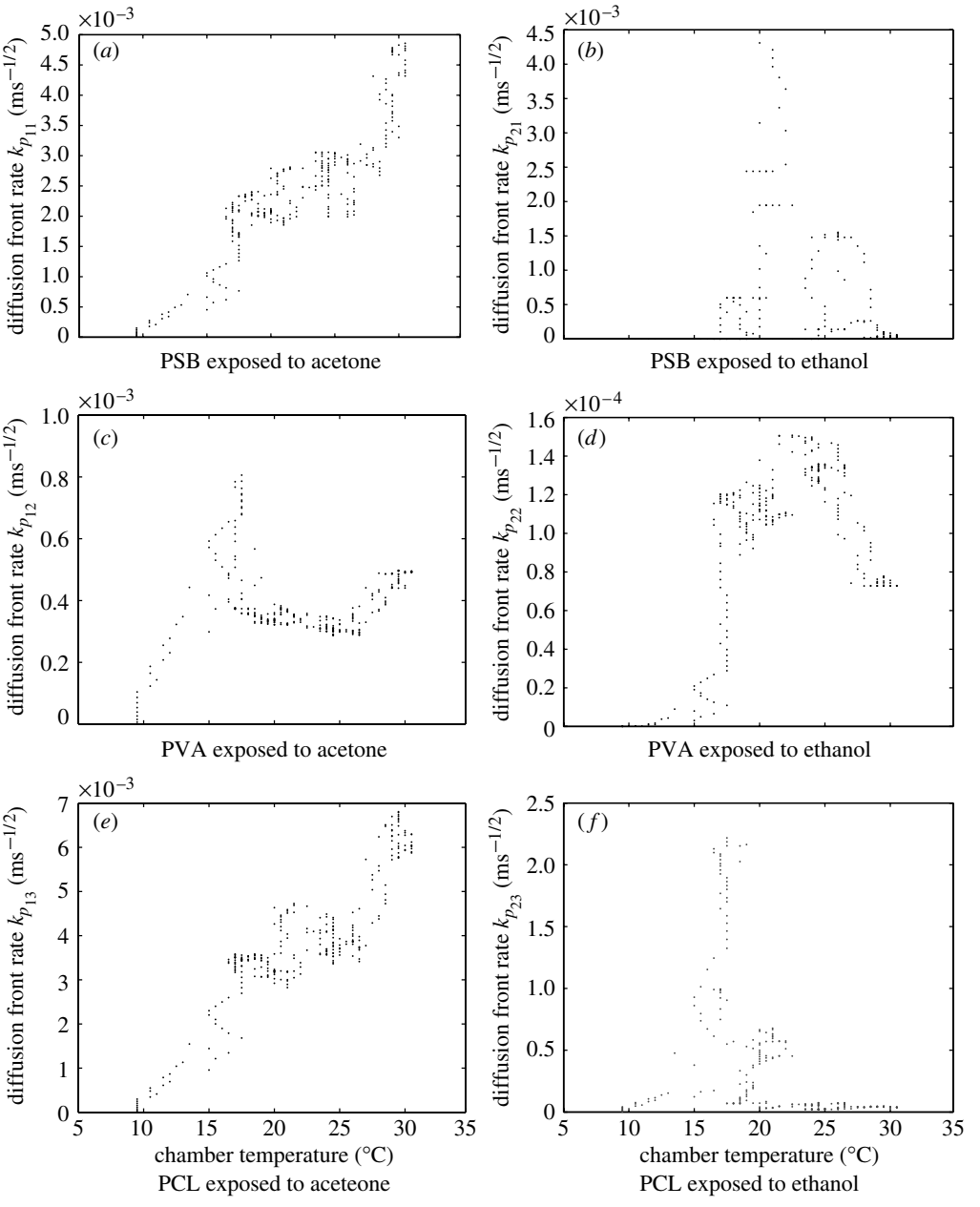

Figure 3. Sensor temperature dependence of diffusion front rate.

Figure 5 shows the dependence of NQc_0 on humidity. Again a variety of different behaviours can be seen between the sensors. The decrease in NQc_0 as humidity increases (shown in figure 4) seems to suggest that the PSB sensor is the most sensitive to water vapour; the lower NQc_0 value means that the response of the sensor has been lowered owing to water absorption.

These results demonstrate the complex interaction of a carbon/polymer-based electronic nose with its environment.

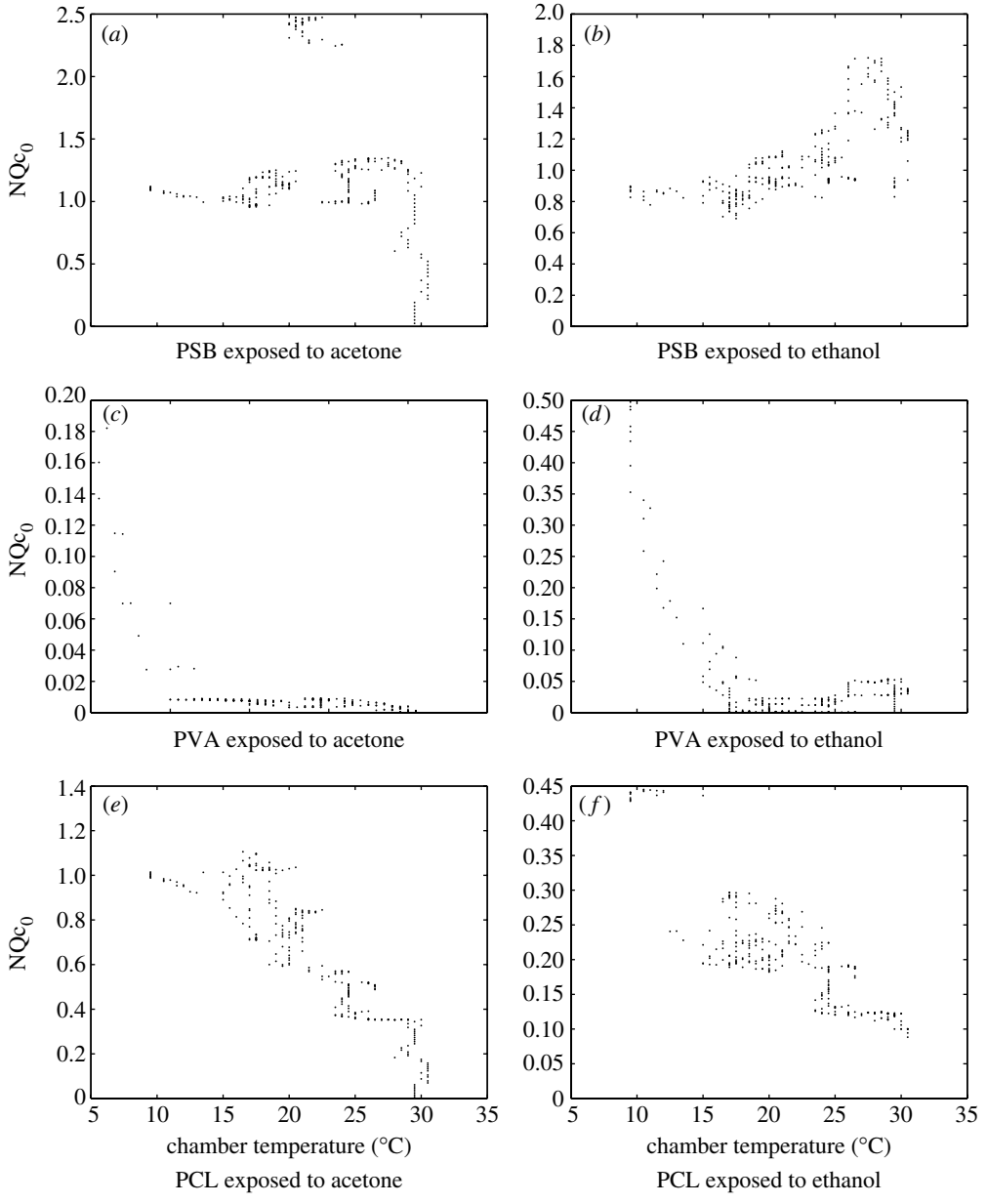

Figure 4. Sensor temperature dependence of NQc_0.

9. Discussion

A novel analytical model is proposed for the response of nanocomposite carbon black/polymer resistive sensors. This model has been successfully fitted to a large number of experimental datasets of sensor data obtained over a wide range of environmental conditions. The resulting estimated parameter values have then been analysed to test for their environmental dependencies. The object of this

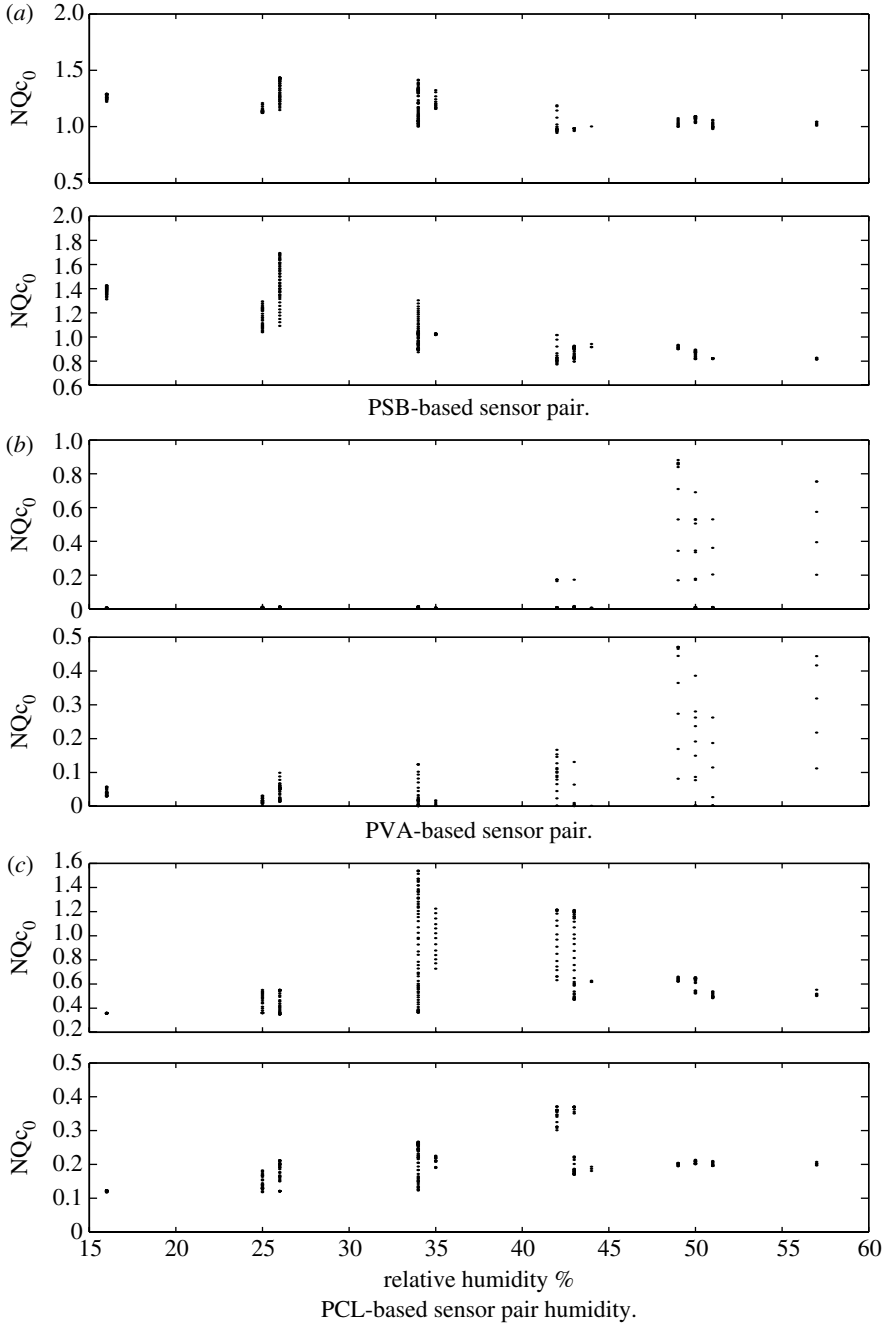

Figure 5. Sensor humidity dependence of NQc_0. For each pair, the upper panel is for acetone while the lower is for ethanol responses.

analysis was to understand more clearly how the dynamics of an electronic nose system is affected by the environment in which it is operating.

The rate at which the sensors react is, as expected, clearly environmentally dependent. The increase in diffusion rate is significantly temperature dependent.

There are two possible effects contributing to this observation. Firstly, mass action is temperature dependent and so reactions will tend to equilibrium more quickly at a higher temperature. Secondly, it is assumed that diffusion is concentration dependent. It is also known that the atmospheric solvent vapour concentration will increase with temperature, so this could also explain the observed behaviour.

The effects of temperature on the parameter product, NQc_0, are very notable and have served to highlight the interaction of processes on the periphery of the electronic nose system. It can be seen that a solvent–polymer interaction can be characterized by the temperature dependence of the device current change. This offers possible design strategies for new electronic nose systems and this has already been investigated in part by Arnold *et al.* (2002). This approach could be broadened to flow aspects (Stitzel *et al.* 2003) and humidity variations. In fact, these ideas are already incorporated in temperature-modulated devices (Ankara *et al.* 2004).

These results also point to the problem of determining an 'optimal' sensor array temperature, which, it would appear, is both solvent and polymer dependent.

There are some disparities between the model and the observed experimental responses. The model predicts more rapid initial dynamics than are actually observed. The reason for this is probably the nature of error in the steady-state approximation, which naturally assumes rapid dynamics. In practice, the flow will not be at a constant velocity with a perfect wavefront. Instead there will be a parabolic flow profile across the channel with some non-laminar mixing. These phenomena would account for the observed initial response being slower than that predicted by our model.

In conclusion, the model fit in figure 2 demonstrates that our mathematical model predicts the behaviour of the real system well with only a 4.5% pointwise error; the environmental dependencies of the model parameters appear, on the whole, to be coherent and corroborated by the previous work. Thus, it can be concluded that this model is a valid approximation of the real system and has successfully analysed the experimental data produced. In this analysis, the chemical and physical aspects of the sensor response have been decoupled by considering the separate processes of solvent transport and the resulting conduction changes in the composite material. This is important because the aim of electronic nose systems is to identify the solvent. The particular solvent will determine the chemical aspects of the response model, not the physical aspects. By decoupling these mechanisms, parameters characterizing the chemical aspects of the system may be used as a better means of solvent, or more generally, odour identification. We believe that this mechanistic modelling approach offers a distinct advantage over data-driven models of chemical sensor arrays and electronic nose systems.

References

Ankara, Z., Kammerer, T., Gramm, A. & Schutze, A. 2004 Low power virtual sensor array based on a micromachined gas sensor for fast discrimination between H_2, CO and relative humidity. *Sens. Actuators B* **100**, 240–245. (doi:10.1016/j.snb.2003.12.072)

Arnold, C., Harms, M. & Goschnick, J. 2002 Air quality monitoring and fire detection with the Karlsruhe electronic micronose KAMINA. *IEEE Sensors* **2**, 179–188. (doi:10.1109/JSEN.2002.800681)

Böttger, H. & Bryksin, V. V. 1985 *Hopping conduction in solids*. Berlin, Germany: Akademie-Verlag.
Carslaw, H. S. & Jaeger, J. C. 1959 *Conduction of heat in solids*. Oxford, UK: Clarendon Press.
Covington, J. A. 2001 CMOS and SOI CMOS FET-based gas sensors. Ph.D. thesis, University of Warwick, UK.
Covington, J. A., Gardner, J. W., Toh, C., Bartlett, P. N., Briand, D. & de Rooij, N. F. 2000 Characterisation of an electrodeposited conducting polymer FET array for vapour and odour sensing. In *Electronic noses and olfaction 2000* (ed. J. W. Gardner & K. C. Persaud). Bristol, UK: Institute of Physics Publishing.
Covington, J. A., Gardner, J. W., Briand, D. & de Rooij, N. F. 2001 A polymer gate FET sensor array for detecting organic vapour. *Sens. Actuators B-Chem.* **77**, 155–162. (doi:10.1016/S0925-4005(01)00687-6)
Crank, J. 1975 *The mathematics of diffusion*. Oxford, UK: Clarendon Press.
Ficker, T. 2003 Non-isotherm steady-state diffusion within glaser's condensation model. *Int. J. Heat Mass Transfer* **46**, 5175–5182.
Flory, P. J. 1953 *Principles of polymer chemistry*. New York, NY: Cornell University Press.
Gardner, J. W. 1989 Electrical conduction in solid-state gas sensors. *Sens. Actuators* **18**, 373–387. (doi:10.1016/0250-6874(89)87043-X)
Gardner, J. W., Llobet, E. & Hines, E. 1998 Pattern recognition techniques in chemical sensing: a review of dynamic modelling. In *9th Int. Conf. Modern Materials and Technologies*, Florence, Italy.
Islam, M. A., Buschatz, H. & Paul, D. 2002 Non-equilibrium surface reactions - a factor in determining steady state diffusion flux. *J. Memb. Sci.* **204**, 370–384. (doi:10.1016/S0376-7388(02)00064-9)
Koscho, M. E., Grubbs, R. H. & Lewis, N. S. 2002 Properties of vapor detector arrays formed through plasticization of carbon black-organic polymer composites. *Anal. Chem.* **74**, 1307–1315. (doi:10.1021/ac011054+)
Marsili-Libelli, S., Guerrizio, S. & Checchi, N. 2003 Confidence regions of estimated parameters for ecological systems. *Ecol. Model.* **165**, 127–146.
Parker, M. A. & Vesely, D. 1986 Temperature and time-dependence of diffusion of PCL into PVC. *J. Polym. Sci. Part B: Polym. Phys.* **8**, 1869–1878. (doi:10.1002/polb.1986.090240821)
Patrash, S. J. & Zellers, E. T. 1993 Characterization of polymeric surface acoustic wave sensor coatings and semiempirical models of sensor responses to organic vapors. *Anal. Chem.* **65**, 2055–2066. (doi:10.1021/ac00063a021)
Rubin, Z., Sunshine, S. A., Heaney, M. B., Bloom, I. & Balberg, I. 1999 Critical behaviour of the electrical transport properties in a tunneling-percolation system. *Phys. Rev. B* **59**, 12 196–12 199.
Stitzel, S. E., Stein, D. R. & Walt, D. R. 2003 Enhancing vapor sensor discrimination by mimicking a canine nasal cavity flow environment. *J. Am. Chem. Soc.* **125**, 3684–3685. (doi:10.1021/ja028239y)
Windie, A. 1984 *Polymer permeability*. Amsterdam, The Netherlands: Elsevier.
Yates, J. W. T. 2004 Black box and mechanistic modelling of electronic nose systems. Ph.D. thesis, University of Warwick, Coventry, UK.